

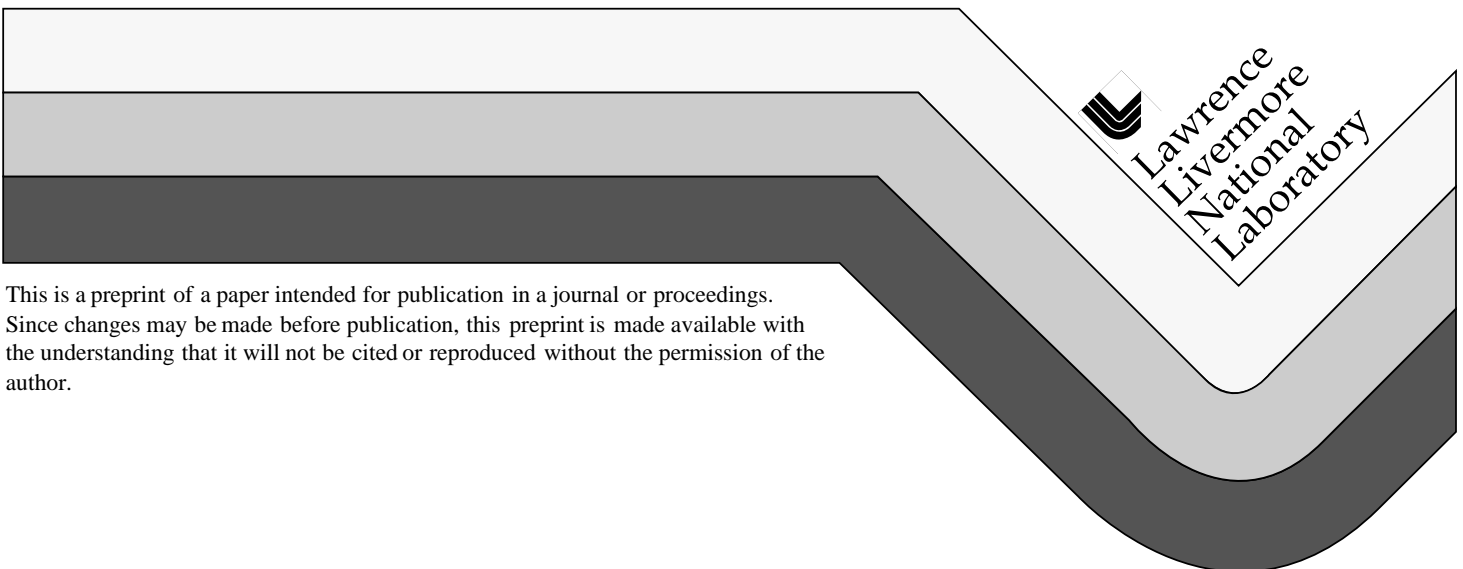
UCRL-JC-132742  
PREPRINT

# **The Effects of Operator Splitting in Computing Curved Shocks**

G. O. Cook, Jr.

This paper was prepared for submittal to the  
1998 Nuclear Explosives Development Conference  
Las Vegas, NV  
October 25-30, 1998

**October 1, 1998**



#### DISCLAIMER

This document was prepared as an account of work sponsored by an agency of the United States Government. Neither the United States Government nor the University of California nor any of their employees, makes any warranty, express or implied, or assumes any legal liability or responsibility for the accuracy, completeness, or usefulness of any information, apparatus, product, or process disclosed, or represents that its use would not infringe privately owned rights. Reference herein to any specific commercial product, process, or service by trade name, trademark, manufacturer, or otherwise, does not necessarily constitute or imply its endorsement, recommendation, or favoring by the United States Government or the University of California. The views and opinions of authors expressed herein do not necessarily state or reflect those of the United States Government or the University of California, and shall not be used for advertising or product endorsement purposes.

## The Effects of Operator Splitting in Computing Curved Shocks

Grant O. Cook, Jr.  
Lawrence Livermore National Laboratory

Dimensionally split numerical methods have been in common use in computational physics for many years. This is due to the need for speed, the formal convergence of Strang splittings, and the accessibility of shock capturing techniques in one dimension. However, the lack of genuinely unsplit multidimensional shock capturing methods has made it difficult to access just how large the errors are in a dimensionally split approach. This applies in spite of splitting corrections that have been used to obtain formally “unsplit” methods. A new class of methods that are genuinely unsplit have recently been developed. These are the so-called “Conservation Element and Solution Element” (CE/SE) methods. Using these high accuracy methods, we show that converging flows and the subsequent expanding flows are accurately captured by CE/SE methods. Contrariwise, it will be shown that dimensionally-split Godunov and unsplit wave propagation methods distort the flow for the same cases, sometimes seriously. (U)

**Keywords:** curved shocks, CE/SE, operator splitting, Godunov, wave propagation

### Introduction

Numerous attempts have been made over the long history of hydrodynamics to accurately simulate shock propagation when the shock is not aligned with the mesh. It is widely held that good results are obtained in the non-aligned case by using methods that are based upon using Strang-type operator splitting (Khan and Liu, 1998; LeVeque, 1997; Saltzman, 1994). With some one-dimensional shock-capturing methods, it has been argued that it is possible to perform fixups to the transverse component of the flow by estimating the error incurred with the operator splitting (Dai and Woodward, 1997; LeVeque, 1997). While we have found that these conclusions are valid if the shocks are weak enough and the flow smooth enough, we have also found that for strong shocks and large curvature situations, operator-split techniques incur large errors.

In this paper, we demonstrate that at least one unique method does not suffer these deficiencies. This method is the Space-Time Conservation Element and Solution Element (CE/SE) method due to Chang (1995). Among its many strengths is that it is genuinely unsplit from the start. It is highly accurate in 2D and 3D, as well as 1D.

In addition to the CE/SE method there is at least one other truly unsplit shock-capturing formalism. It is the Riemann Invariant Manifold theory (Papalexandris et al., 1997) which can be used with a variety of one-dimensional methods. This approach will not be considered further here.

Some of the unique aspects of the CE/SE method are:

- No directional splitting is employed in 2D and 3D.

- It solves the integral form of conservation laws in the space-time domain.
- It conserves space-time flux locally and globally.
- A leap-frog time advance mechanism is used. Because of this, flow information on interfaces separating conservation elements can be evaluated without interpolation or extrapolation.
- In addition to the flow variables, the time derivative and several spatial derivatives of the flow variables are treated as dependent variables. This means that the flow structure is not calculated through a reconstruction procedure as in Godunov schemes.
- When dissipation is added to suppress wiggles, it is a linear addition to the non-dissipative spatial derivatives of the flow variables. Dissipation is not directly added to the flow variables.

Notably, shock capture is achieved without a characteristic decomposition or the need to solve a Riemann problem.

We will begin by sketching the essentials of the CE/SE method. Then the test problems representing converging and diverging 2D shocks are introduced. All of the problems were run on uniform square Cartesian grids. The results obtained with the CE/SE method are then compared with those found from two (dimensionally-split) Godunov methods.

### The CE/SE Method

Chang and his coworkers have shown that the propagation of signals in hyperbolic conservation laws implies that it is beneficial to formulate the solution process as a leapfrog method (Chang, 1995). It is easy to select conservation elements to allow a leapfrog update. Each conservation element (CE) is a region in space-time over which the integral form of each conservation law is valid. Conservation elements are chosen to fill in the space-time problem domain. While many choices are possible, we choose rectangular brick volumes in space-time for the conservation elements in the simulation code used here.

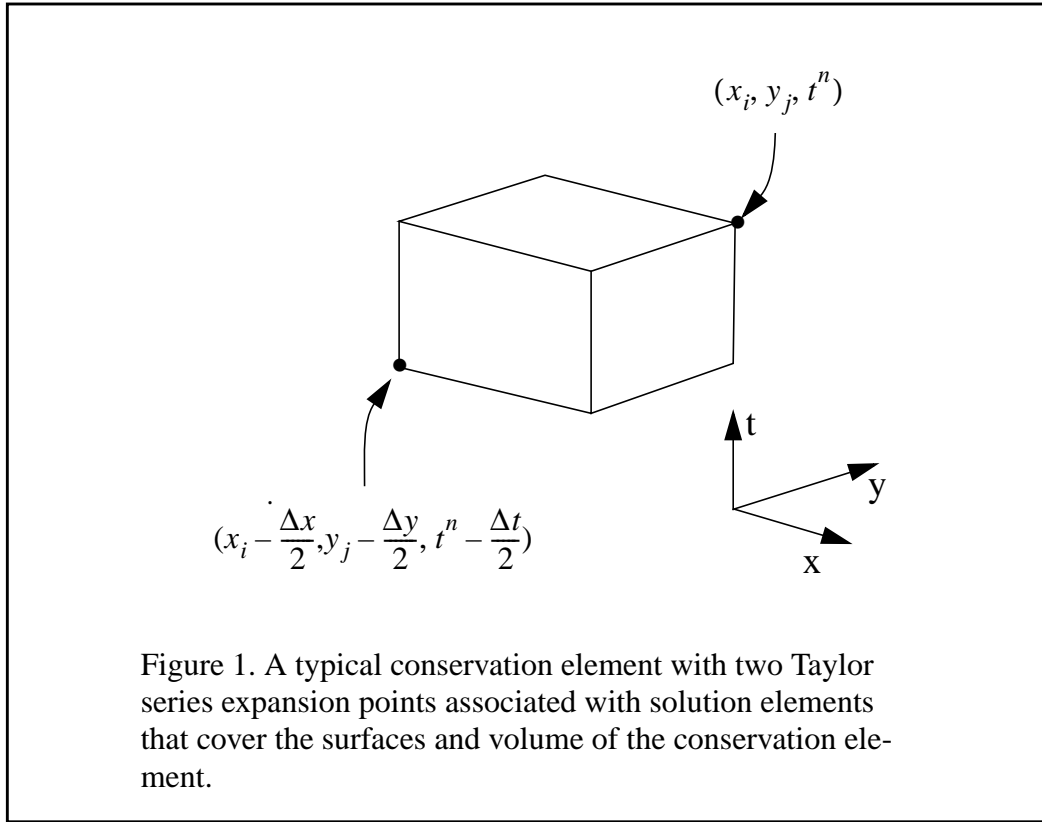
Next, the solution elements (SE) are selected as the domains over which values of the dependent variables are needed in integrals arising from the integral form of the conservation laws. In these domains a convenient representation for the dependent variables is selected. Usually, this is a Taylor series representation that is expanded about a center point in the solution element. For instance, in two dimensions on a rectangular grid that lines up with the coordinate axes, we pick the following representation for a dependent variable  $g$ .

$$\begin{aligned}
 g(x, y, t, x_i, y_j, t^n) = & g_{i,j}^n + \left( \frac{\partial g}{\partial t} \right)_{i,j}^n (t - t^n) \\
 & + \left( \frac{\partial g}{\partial x} \right)_{i,j}^n (x - x_i) + \left( \frac{\partial g}{\partial y} \right)_{i,j}^n (y - y_j) + \left( \frac{\partial^2 g}{\partial x \partial y} \right)_{i,j}^n (x - x_i)(y - y_j)
 \end{aligned} \tag{1}$$

Note that  $n$  denotes a time level,  $i$  denotes an index in the  $x$  direction, and  $j$  an index in the  $y$

direction. These indices specify the center point of the solution element that is the domain of validity for equation 1.

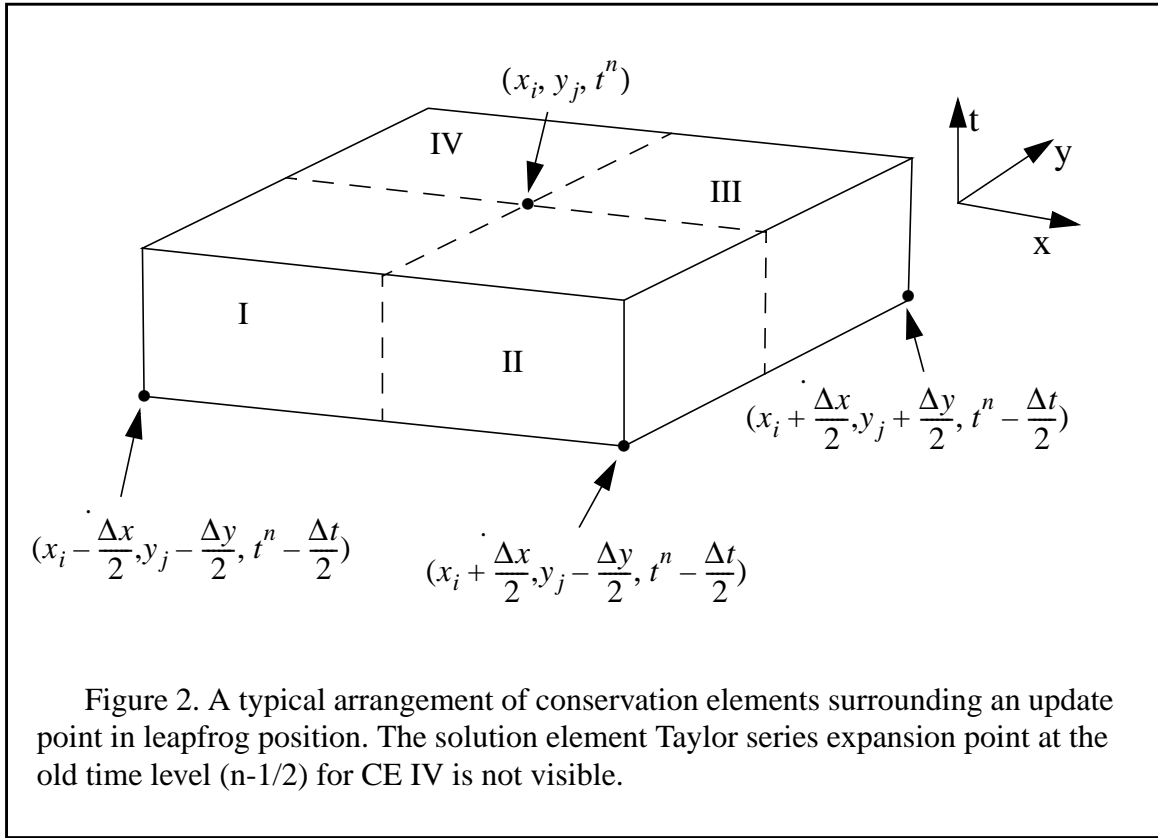
As shown in Figure 1, typically two solution elements are involved in the integration of a conservation law over a CE. The expansion points for the Taylor series in each solution element are denoted by the bullet symbol. One of these solution elements involves known quantities from the past time level. The other solution element is that for the unknown advanced-time values of the coefficients in the corresponding Taylor series.



In the Taylor series expansion,  $\left(\frac{\partial g}{\partial t}\right)_{i,j}^n$  is determined from the partial differential equation for  $g$ . The remaining four unknowns,  $g_{i,j}^n$ ,  $\left(\frac{\partial g}{\partial x}\right)_{i,j}^n$ ,  $\left(\frac{\partial g}{\partial y}\right)_{i,j}^n$ , and  $\left(\frac{\partial^2 g}{\partial x \partial y}\right)_{i,j}^n$  are found by solving the four equations obtained by integrating the conservation law for  $g$  over the four individual conservation elements surrounding the update point  $(x_i, y_j, t^n)$ . Figure 2 shows the four conservation elements that surround a given update point in a uniform rectangular Cartesian coordinate system. The CE labelled I is the same CE illustrated in Figure 1. This sketch also makes it a little clearer how one leapfrog time step works. It also motivates the fact that when the integrals for two adja-

cent CEs are added together, the contribution on the common face is zero.

Note that no dissipation is involved in obtaining these coefficients in the Taylor series. Of course, in order to prevent ringing at shock fronts, dissipation must be added to the non-dissipative solution. Originally, Chang used a two parameter dissipation model for damping this ringing. By treating the CE of dissipation model as the union of the CEs surrounding an update point  $(x_i, y_j, t^n)$ , a method for conservatively modifying the derivative coefficients was obtained. Recently, Chang refined this technique with a three parameter dissipation model (Chang, 1998).



The basic idea behind this new dissipation model is to separately damp weak waves and strong shocks. This is indicated in equation 2, where  $\epsilon$  is the parameter for damping weak waves and  $\beta$  is the parameter for damping shocks.

$$g_x^{\text{diss}} = g_x^{\text{non-diss}} + 2\epsilon(g_x^c - g_x^{\text{non-diss}}) + \beta(g_x^w - g_x^c), \quad (2)$$

where  $g_x^c$  is a central difference approximation to  $g_x$ ,  $g_x^w$  is a nonlinear weighted average of one-sided approximations to  $g_x$ , and

$$g_x^{\text{non-diss}} = \left. \frac{\partial g}{\partial x} \right|_{CE}, \quad (3)$$

is the solution obtained for  $\left(\frac{\partial g}{\partial x}\right)_{i,j}^n$  when solving the four equations obtained from integrating over the CEs I, II, III, and IV in Figure 2.

In order to compute  $g_x^c$  and  $g_x^w$ , it is first necessary to obtain some advanced-time estimates from the previous time level data. To accomplish this, the Taylor series is used:

$$g_{i\pm\frac{1}{2},j\pm\frac{1}{2}}^n \approx g_{i\pm\frac{1}{2},j\pm\frac{1}{2}}^{n-\frac{1}{2}} + \frac{\Delta t}{2} \left( \frac{\partial g}{\partial t} \right)_{i\pm\frac{1}{2},j\pm\frac{1}{2}}^{n-\frac{1}{2}}. \quad (4)$$

$g_x^c$  is found from these values as follows:

$$g_x^c = \frac{\frac{1}{2} \left( g_{i+\frac{1}{2},j+\frac{1}{2}}^n + g_{i+\frac{1}{2},j-\frac{1}{2}}^n \right) - \frac{1}{2} \left( g_{i-\frac{1}{2},j+\frac{1}{2}}^n + g_{i-\frac{1}{2},j-\frac{1}{2}}^n \right)}{\Delta x} \quad (5)$$

Coupling  $g_{i\pm\frac{1}{2},j\pm\frac{1}{2}}^n$  with the known value at the update point,  $g_{i,j}^n$ , four planes can be constructed, one in each of the  $\pm x$  and  $\pm y$  directions. For the  $i^{\text{th}}$  such plane, the  $x$  and  $y$  derivatives of  $g$  can be computed. Then, if  $g_x^{(i)}$  and  $g_y^{(i)}$  are the derivatives on the  $i^{\text{th}}$  plane, define

$$\theta_i = \sqrt{(g_x^{(i)})^2 + (g_y^{(i)})^2}. \quad (6)$$

With this quantity, the nonlinear weighted average of  $g_x$  can be defined as:

$$g_x^w = \frac{(\theta_2\theta_3\theta_4)^\alpha g_x^{(1)} + (\theta_1\theta_3\theta_4)^\alpha g_x^{(2)} + (\theta_1\theta_2\theta_4)^\alpha g_x^{(3)} + (\theta_1\theta_2\theta_3)^\alpha g_x^{(4)}}{(\theta_2\theta_3\theta_4)^\alpha + (\theta_1\theta_3\theta_4)^\alpha + (\theta_1\theta_2\theta_4)^\alpha + (\theta_1\theta_2\theta_3)^\alpha} \quad (7)$$

with  $\alpha$  usually chosen to be 1.0 or 2.0.  $g_y^w$  is computed analogously. This limiter is the generalization for a regular rectangular grid of Chang's two-dimensional limiter on a regular triangular grid (Chang et al., 1995).

It is also important to note that  $g_x^w$  is computed in a way that introduces no directional bias. This generalized multidimensional limiter preserves the genuinely unsplit nature of the CE/SE method. Thus, unlike techniques based upon Godunov or Riemann solvers, there are no fixups or adjustments required to accommodate coupling between different directions.

It is most common to use an artificial viscosity as a way of adding dissipation to a physical model. Since an artificial viscosity is added to the physical pressure, it is therefore the case that linear changes in the artificial viscosity introduce nonlinear changes in the solution. By contrast, the CE/SE dissipation model introduces changes in the derivative coefficients that are linear in the amount of dissipation added. Furthermore, the dissipation is added only after the non-dissipative solution is computed. Chang found that the addition of this dissipation breaks the space-time invariance properties that a non-dissipative CE/SE method possesses (Chang, 1995).

The overall result is that the CE/SE model provides better control of the dissipation than methods that introduce dissipation inside of a nonlinear operator. The CE/SE dissipation model also yields more readily to mathematical analysis.

### Applying the CE/SE Method to the Two-Dimensional Euler Equations

For the two dimensional Euler equations in Cartesian coordinates, we solve the equations in internal energy form. That is, the dependent variables are chosen to be  $(\rho, \rho v_x, \rho v_y, e_{\text{int}})$ . We choose to denote the  $x$  and  $y$  components of the momentum by  $p_x$  and  $p_y$ ; that is,  $p_x = \rho v_x$  and  $p_y = \rho v_y$  respectively. Also, the symbol  $P$  denotes the pressure, and should not be confused with the components of the momentum vector.

We illustrate the application of the CE/SE method to this situation by examining the conservation law for  $p_y$ . The first step is to write the integral form of the conservation law for  $p_y$  beginning with equation 8:

$$\int_{x_i}^{x_i + \frac{\Delta x}{2}} \int_{y_j}^{y_j + \frac{\Delta y}{2}} \int_{t^n - \frac{\Delta t}{2}}^{t^n} \left( \frac{\partial p_y}{\partial t} + \frac{\partial}{\partial x} \left( \frac{p_x p_y}{\rho} \right) + \frac{\partial}{\partial y} \left( P + \frac{p_x^2}{\rho} \right) \right) dx dy dt = 0 \quad (8)$$

Because of the use of conservation form, the three terms can be integrated once as shown in expressions 9, 10, and 11. Note that the term in each equation that is not at the update point uses old time level data (at  $t = t^n - \frac{\Delta t}{2}$ ).

$$\int_{x_i}^{x_i + \frac{\Delta x}{2}} \int_{y_j}^{y_j + \frac{\Delta y}{2}} ((p_y)^n - (p_y)^{n-1/2}) dx dy \quad (9)$$

$$\int_{y_j}^{y_j + \frac{\Delta y}{2}} \int_{t^n - \frac{\Delta t}{2}}^{t^n} \left( \left( \frac{p_x p_y}{\rho} \right) \Big|_{i+1/2} - \left( \frac{p_x p_y}{\rho} \right) \Big|_i \right) dy dt \quad (10)$$

$$\int_{x_i}^{x_i + \frac{\Delta x}{2}} \int_{t^n - \frac{\Delta t}{2}}^{t^n} \left( \left( P + \frac{p_x^2}{\rho} \right) \Big|_{j+1/2} - \left( P + \frac{p_x^2}{\rho} \right) \Big|_j \right) dx dt \quad (11)$$

Now define the two flux terms in equation 8 as:

$$F_{i,j}^n = \frac{(p_x)_{i,j}^n (p_y)_{i,j}^n}{\rho_{i,j}^n} \quad G_{i,j}^n = P_{i,j}^n + \frac{(p_x^2)_{i,j}^n}{\rho_{i,j}^n} \quad (12)$$

The Taylor series for  $p_y$  can be used to evaluate the integrals in expression 9. In order to obtain comparable results in the integrals in expressions 10 and 11, one choice is to linearize the flux terms as in equations 13 and 14.

$$F(y, t, i, j, n) = F_{i,j}^n + \left( \frac{\partial F}{\partial t} \right)_{i,j}^n (t - t^n) + \left( \frac{\partial F}{\partial y} \right)_{i,j}^n (y - y_j) \quad (13)$$

$$G(x, t, i, j, n) = G_{i,j}^n + \left( \frac{\partial G}{\partial t} \right)_{i,j}^n (t - t^n) + \left( \frac{\partial G}{\partial x} \right)_{i,j}^n (x - x_i) \quad (14)$$

In evaluating  $\frac{\partial F}{\partial t}$  and  $\frac{\partial G}{\partial t}$ , the time derivatives of the dependent variables are encountered.

Just as  $\left( \frac{\partial p_y}{\partial t} \right)_{i,j}^n$  in the Taylor series for  $p_y$  is replaced by its value from the differential equation

that defines it, each time derivative in  $\frac{\partial F}{\partial t}$  and  $\frac{\partial G}{\partial t}$  is replaced by the corresponding differential equation definition. This process is repeated for the conservation integrals over CE<sub>I</sub>, CE<sub>II</sub>, and

CE<sub>IV</sub>. Thereby, we obtain four equations to solve for  $(p_y)_{i,j}^n$ ,  $\left( \frac{\partial p_y}{\partial x} \right)_{i,j}^n$ ,  $\left( \frac{\partial p_y}{\partial y} \right)_{i,j}^n$ , and  $\left( \frac{\partial^2 p_y}{\partial x \partial y} \right)_{i,j}^n$ .

Because the grid is uniform in this case, if the results of integrating over the four CEs are added together, we obtain an expression that depends only upon  $p_y$ , and not on any of its derivatives.

Consequently, the dependent variables can be partially updated on this grid without the need for solving a system of equations. When  $\varepsilon = \frac{1}{2}$ , it is not necessary to solve for the non-dissipative

derivative coefficients. However, this is a large amount of dissipation; so, for higher accuracy, it is recommended to solve three of the  $p_y$  equations for the derivative coefficients. When integrating internal energy equation over a CE, nonlinear terms are found due to the cross derivatives of kinetic energy terms. Hence, in this case, a nonlinear solver is required to solve the full system of equations. Happily, the nonlinearity is weak, so functional iteration works well given a good starting guess.

It is of interest to compare actual implementations of the CE/SE method and a Godunov method. Our CE/SE implementation on rectangular grids with  $\varepsilon = \frac{1}{2}$  and  $\beta = 1$  is faster per

major time step (two leapfrog steps in a major time step) than the Godunov solver. Also, we observed that the CE/SE implementation is able to get reliable solutions at larger time steps than the Godunov method. These observations have been made in a framework where both the CE/SE method and a Godunov method are implemented in the same simulation code, and in a way so that both use exactly the same underlying simulation code services (such as initialization, memory management, graphics, etc.). Consequently, the algorithms themselves can be directly compared for speed, accuracy, code size, etc. Since the CE/SE method involves solving for the flow variables and their gradients, it is not obvious how this can be made to be more efficient than an optimized Godunov solver. This achievement was made possible through the use of advanced symbolic computing tools for the bulk of the coding, very sophisticated optimization, and clever adjustments to the multidimensional limiters.

When reducing the amount of dissipation used by CE/SE, a nonlinear solver is required, and the CE/SE method then slows down to about half the speed of the Godunov solver. Considering the gains in accuracy, especially for curved features, this is an easily justified cost.

### Test Problems

We illustrate curved shock issues with converging cylindrical shocks. In order to elucidate the problems that arise due to split versus unsplit methods, we pick model problems in cylindrical coordinates that depend only upon the radial coordinate. The simulation is then performed on a uniform two-dimensional rectangular Cartesian grid that lies in the  $(\rho, \theta)$  cylindrical coordinate plane. The size of the grid is 128 by 128.

In the two problems considered here, the initial conditions include features that do not conform to the geometry of the grid. Hence, stairstepping errors or mesh imprinting occurs due to the initial conditions. Nonetheless, as will be seen from the CE/SE solutions, these errors are small.

The first Godunov solver used in these simulations is based upon the Direct Eulerian MUSCL scheme.<sup>4</sup> It employs a standard ADI-type approach for solving the multidimensional Euler equations; that is, after solving a sequence of Riemann problems in one direction, it performs transverse fixups in the directions normal to the sweep. In order to remove some bias, the order of directional sweeps is reversed from one-half time step to the next. Since this solver is the Godunov method implemented in the Odyssey code, it will be identified as the Odyssey Godunov solver in the following discussion.

The second Godunov solver employed is one in the CLAWPACK package as embedded in AMR-CLAW.<sup>7</sup> Of those available, we selected the default Godunov technique employed in the Euler example section of CLAWPACK. It is a wave propagation method with an ‘unsplit’ character in the sense that it approximates the terms that are missing in the operator splitting of the full (non-linear) Euler equations.

The CE/SE solver used in the simulations used the following parameter values for the dissipation model:  $\varepsilon = 0.25$  and  $\beta = 0.12$ , with  $\alpha = 1.0$  in the first problem and  $\alpha = 2.0$  in the second problem. Six digits of accuracy in the nonlinear solver was requested in each case.

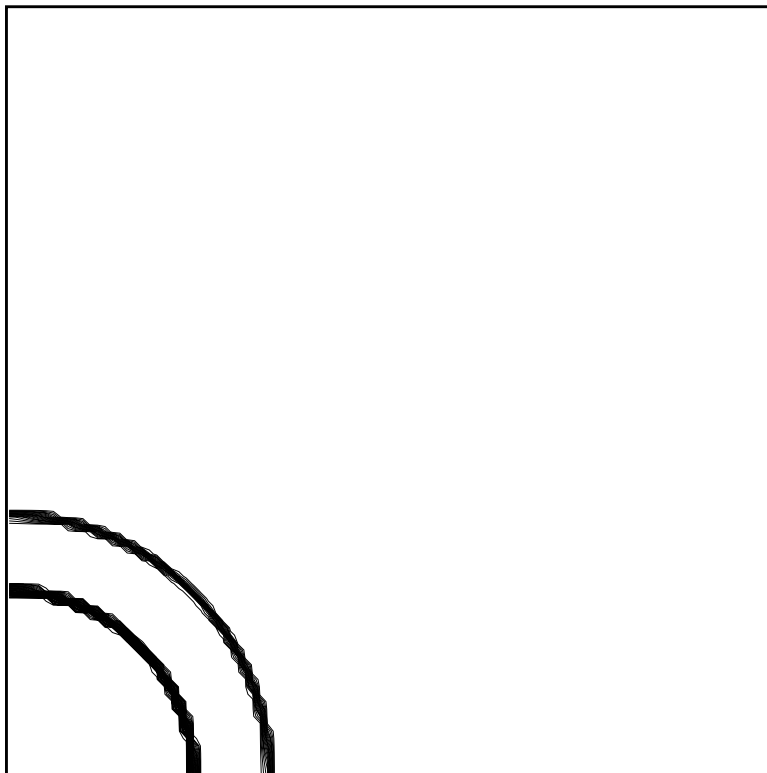


Figure 3. Initial conditions for the three region problem. The inner very low density region has a low pressure; the low density outer region has a high pressure; and the high density middle region has an intermediate pressure.

All regions in these problems are made up of  $\gamma$ -law gases with  $\gamma = \frac{5}{3}$ .

The first problem is a three region problem where the inner region is very low density, low pressure, the middle region is higher density and medium pressure, while the outer region is low density and high pressure. Each region is bounded by cylindrical surfaces. The initial density contours are shown in Figure 3. Note from the Godunov solutions in Figures 4 and 5 that just before the main shock reaches the lower left corner of the plot, the Odyssey Godunov result is showing hints of flattening in the solution along the diagonal of the grid (where  $x=y$ ,  $x$  and  $y$  being the two Cartesian coordinates)). In the CLAWPACK solution, the flattening is very pronounced. A short while after the main shock bounce is seen in Figures 6 and 7. A significant deterioration of both Godunov solutions near the origin has clearly occurred. In fact, in addition to flattening of

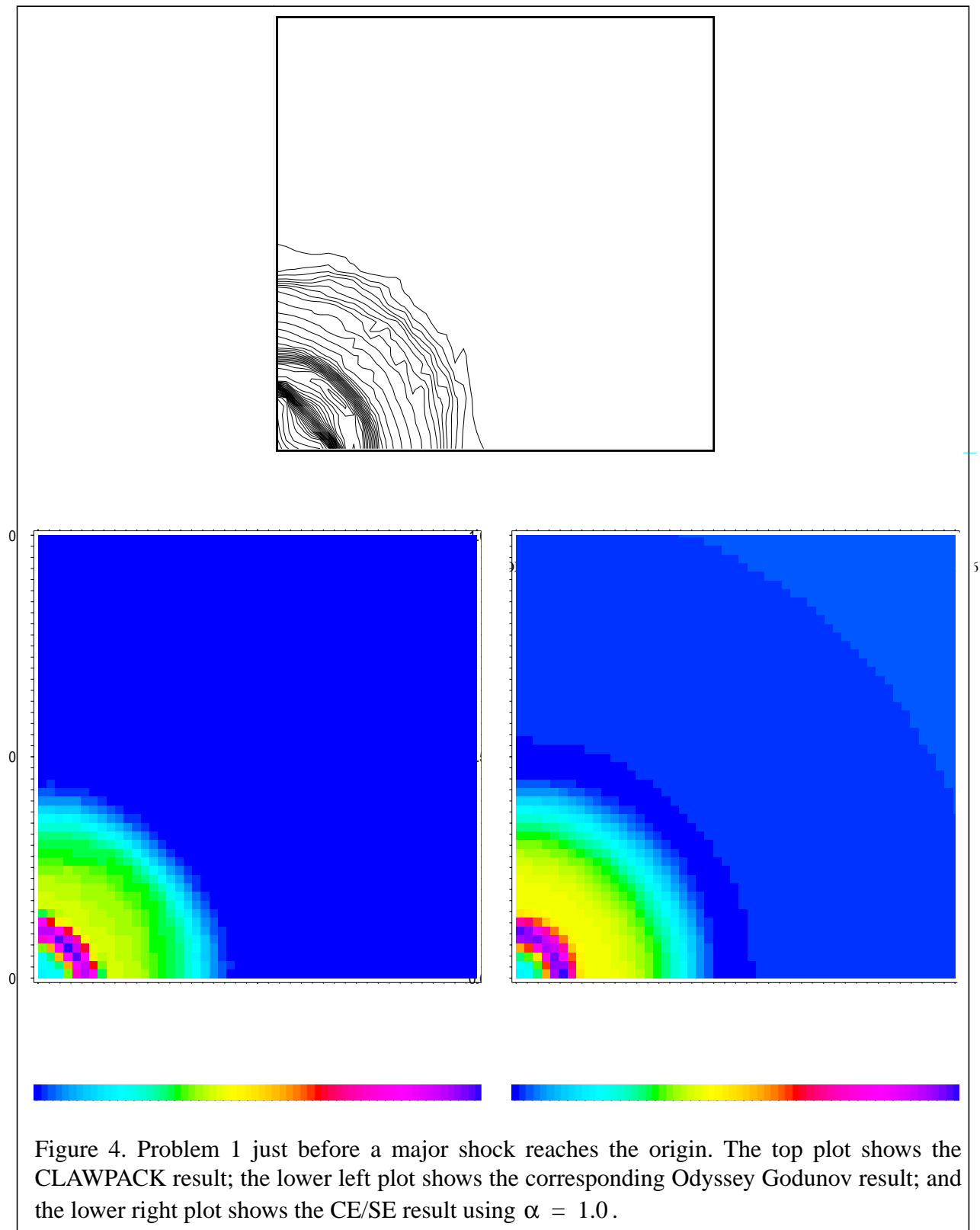
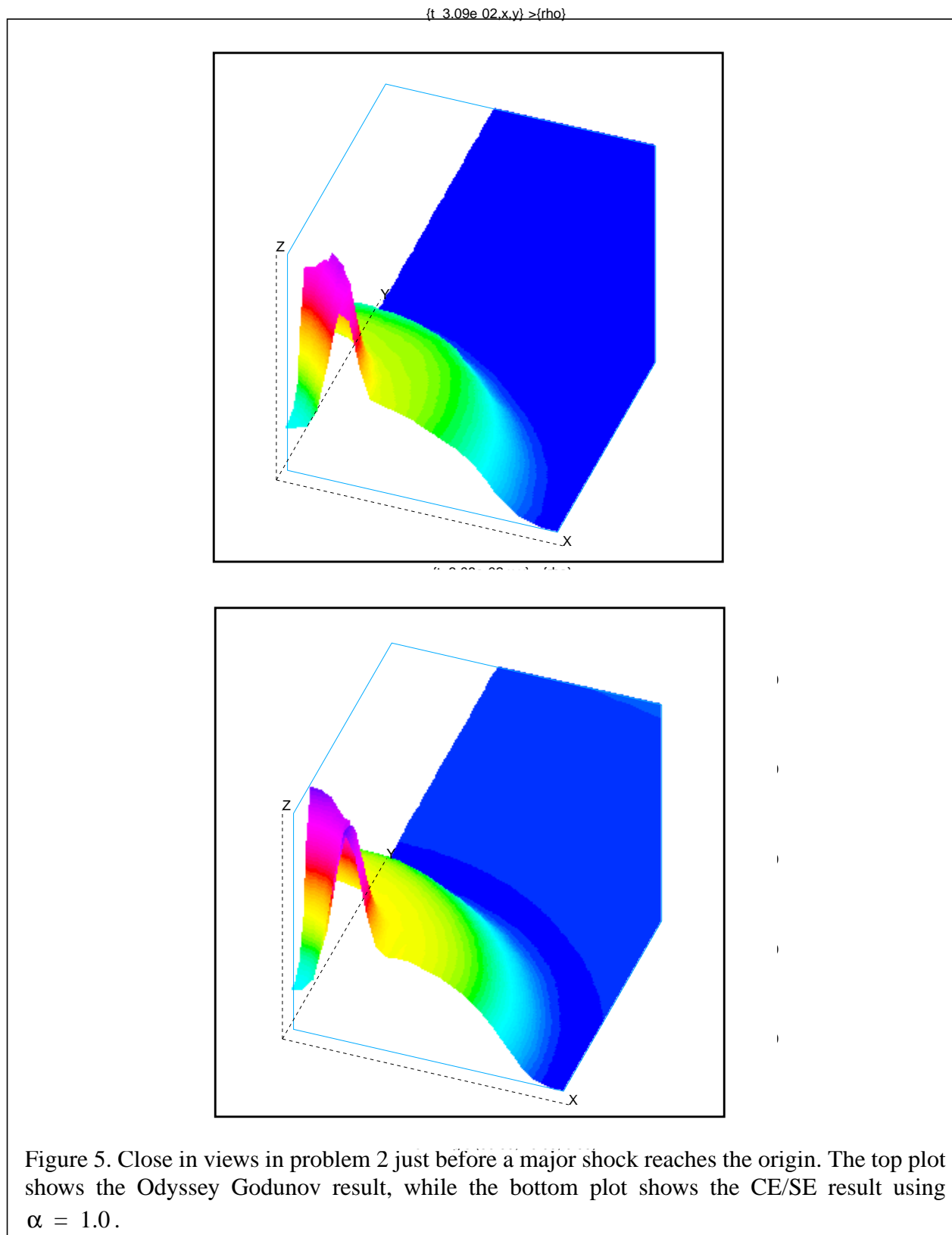
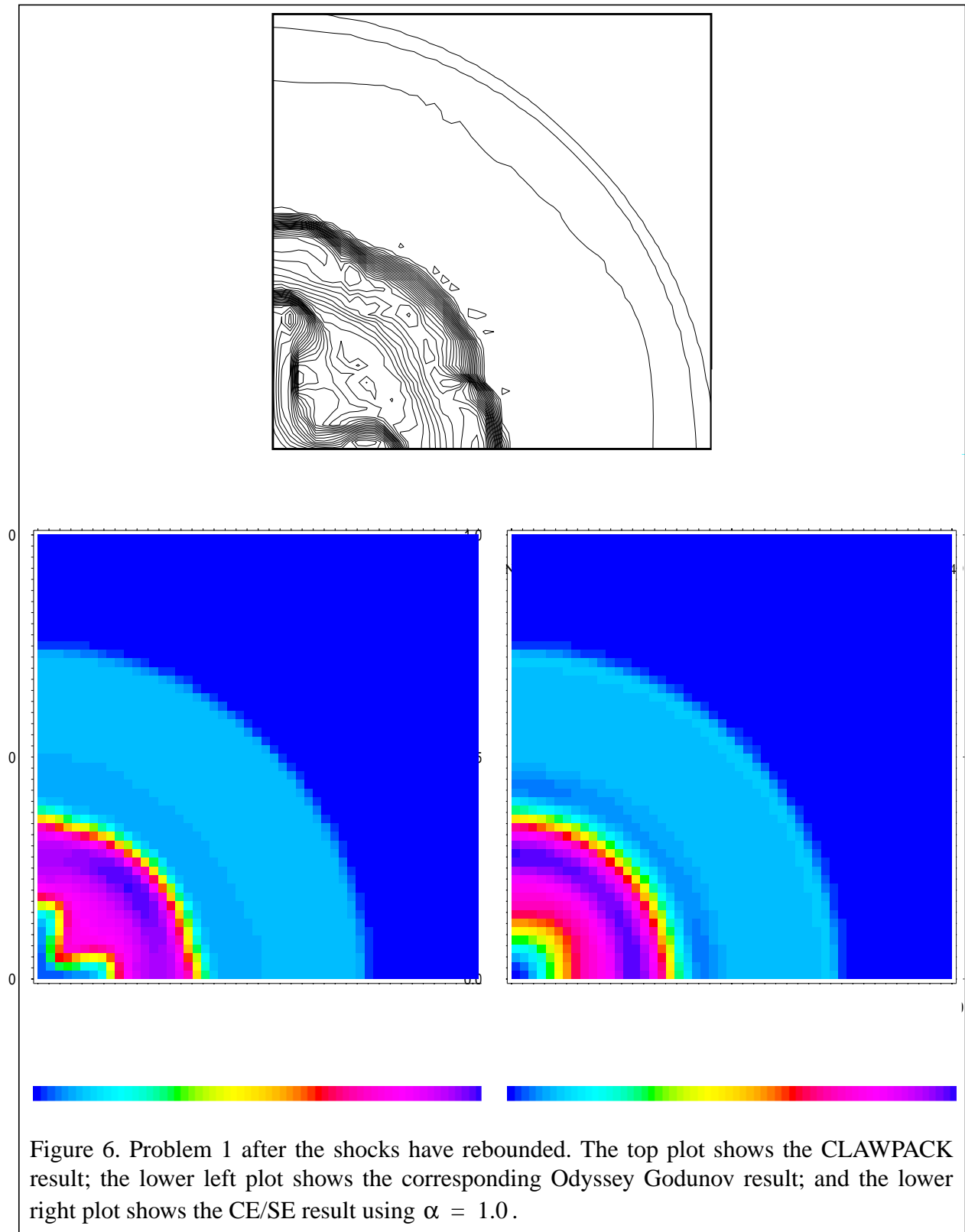
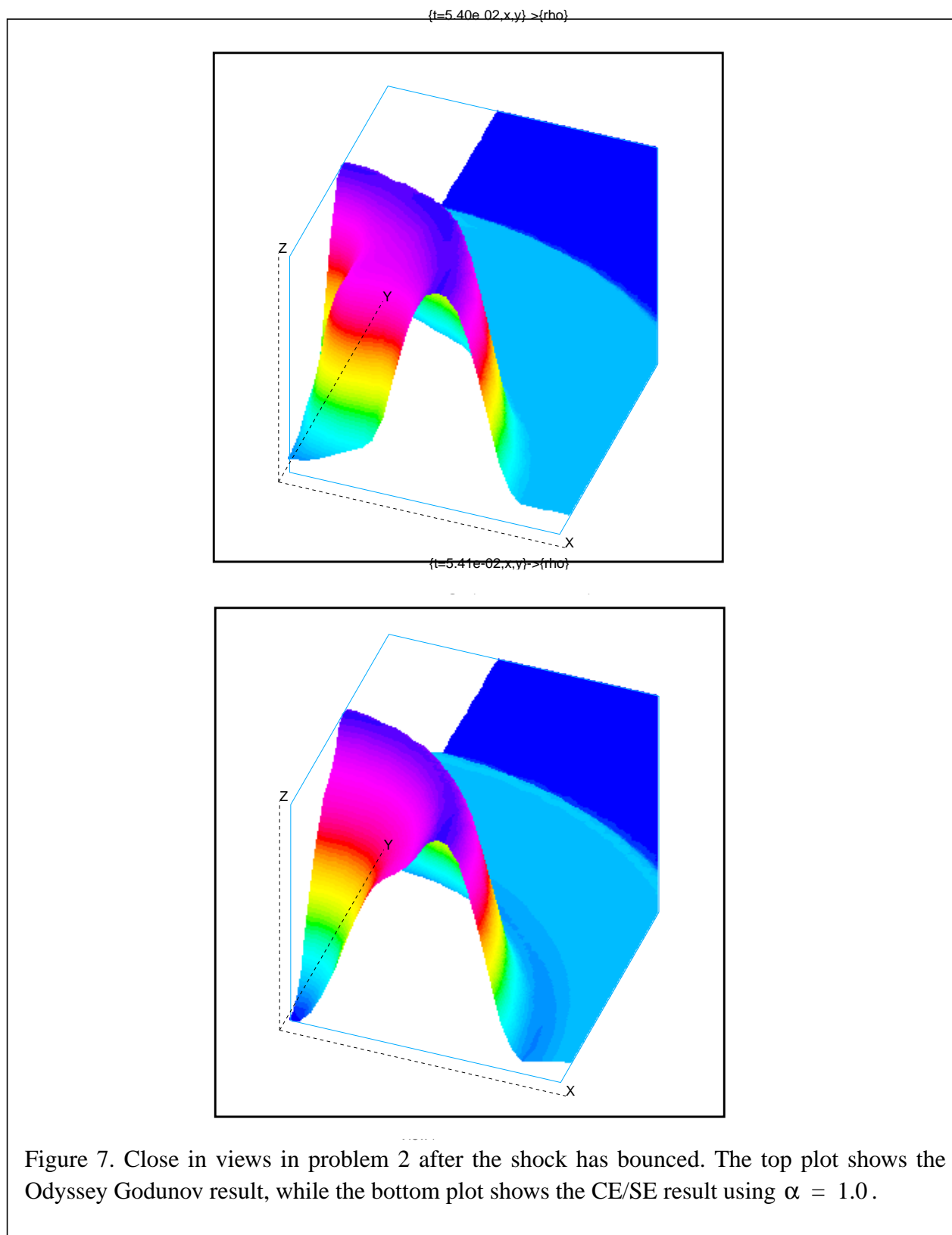


Figure 4. Problem 1 just before a major shock reaches the origin. The top plot shows the CLAWPACK result; the lower left plot shows the corresponding Odyssey Godunov result; and the lower right plot shows the CE/SE result using  $\alpha = 1.0$ .







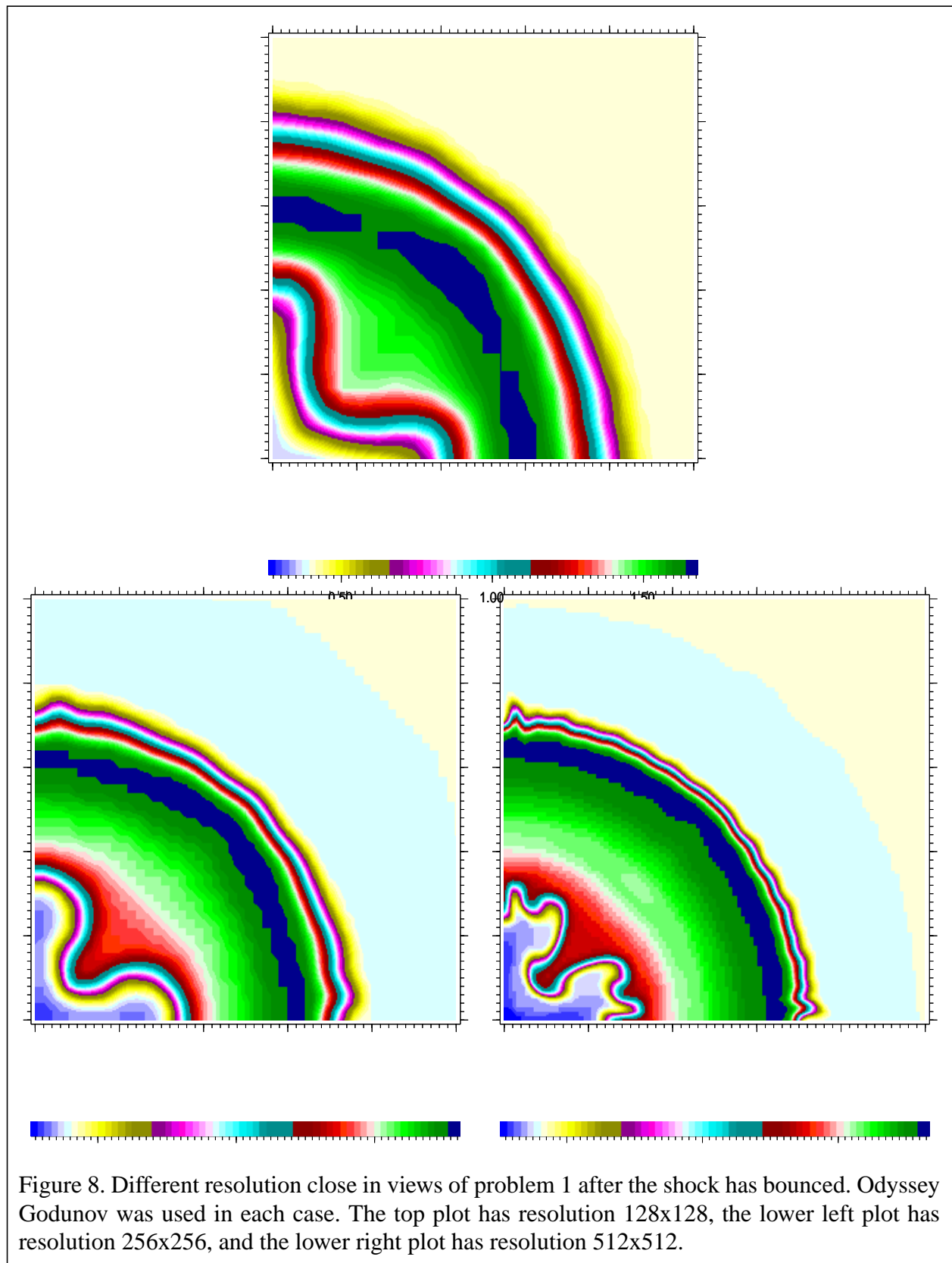
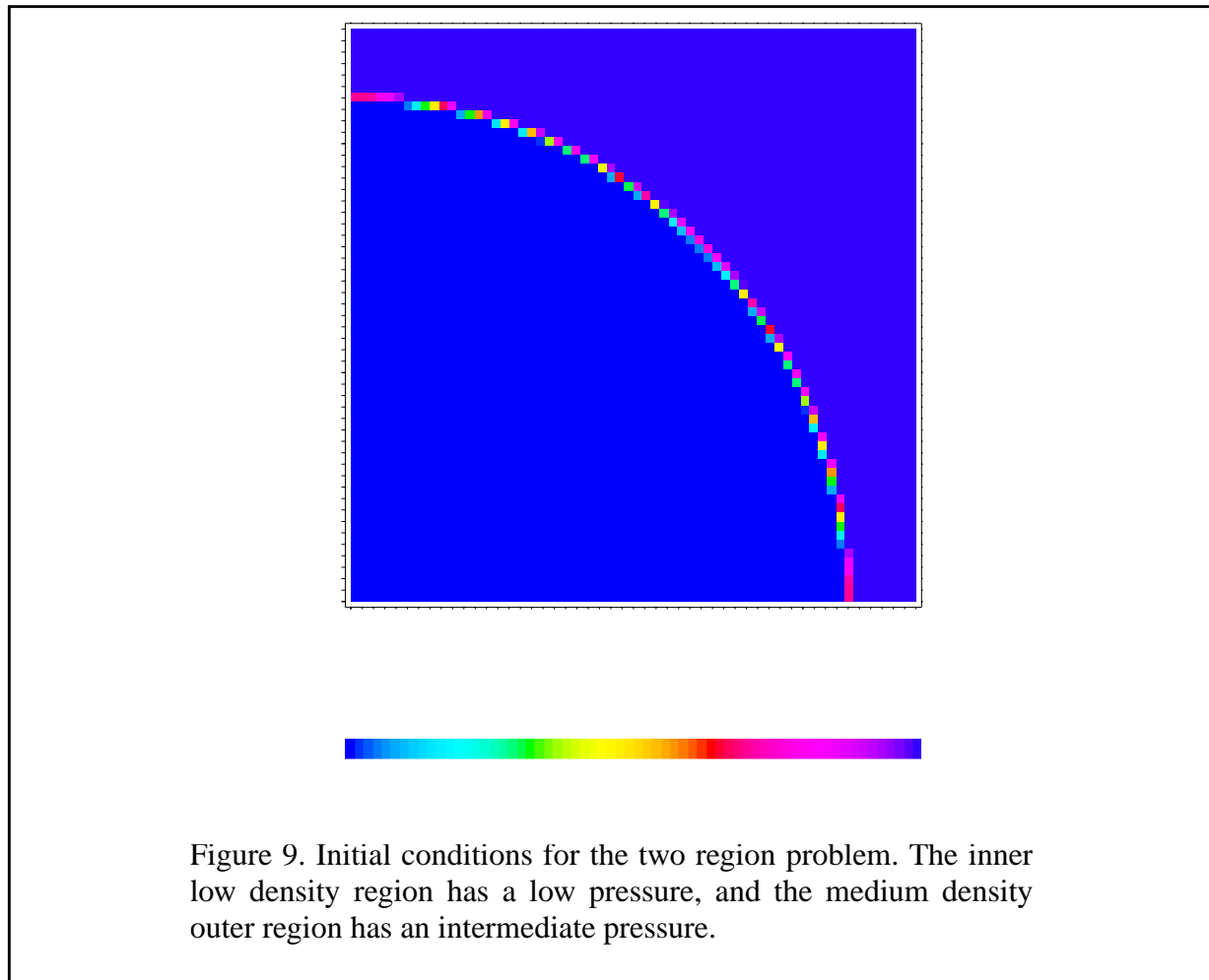


Figure 8. Different resolution close in views of problem 1 after the shock has bounced. Odyssey Godunov was used in each case. The top plot has resolution 128x128, the lower left plot has resolution 256x256, and the lower right plot has resolution 512x512.



the shocks, there appears to be jetting occurring on the coordinate axes near the origin. In the case of CE/SE, there is slight squaring of the contours out a short distance from the origin. Also, a minor manifestation of the mesh imprinting of the initial conditions is visible. But overall, the CE/SE solution is excellent.

It is tempting to speculate that one only need refine the mesh to help the operator split technique overcome its difficulty. The results in Figure 8 demonstrate clearly that we are nowhere close to the convergence limit of the Strang-type splitting for this problem. In fact, more problems are being introduced through refinement.

The second problem is a two region problem where the inner region is a low density, low pressure gas, and the outer region is a medium density and medium pressure gas. Once again, the regions are bounded by a cylindrical surface. Contours of this setup are shown in Figure 9.

From Figures 10 and 11, just before the main shock reaches the lower left corner of the plot, slight hints of flattening appear in the Godunov solutions along the diagonal of the grid occurs. The effect is not as strong as in the first problem. However, color contour plots definitely reveal the

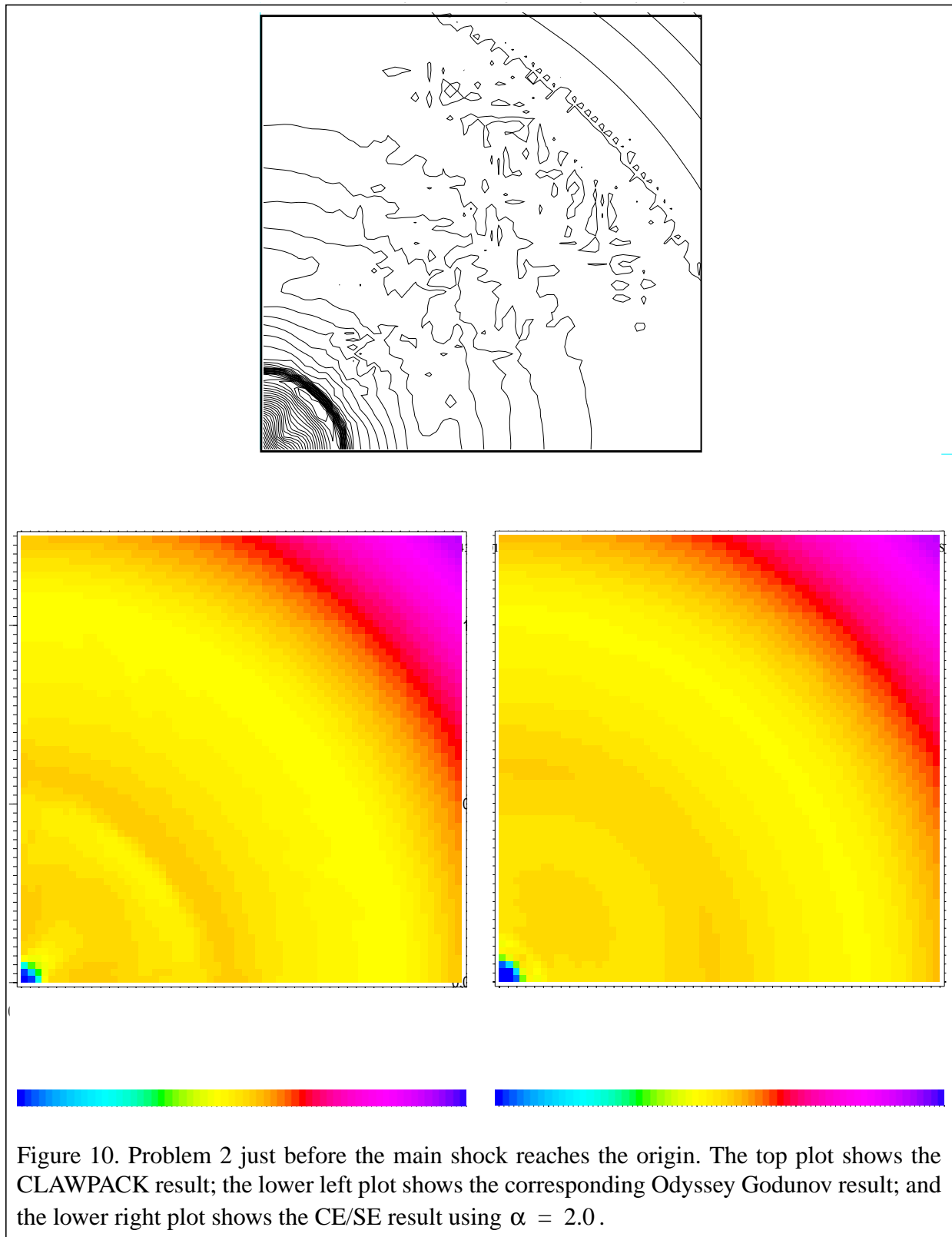


Figure 10. Problem 2 just before the main shock reaches the origin. The top plot shows the CLAWPACK result; the lower left plot shows the corresponding Odyssey Godunov result; and the lower right plot shows the CE/SE result using  $\alpha = 2.0$ .

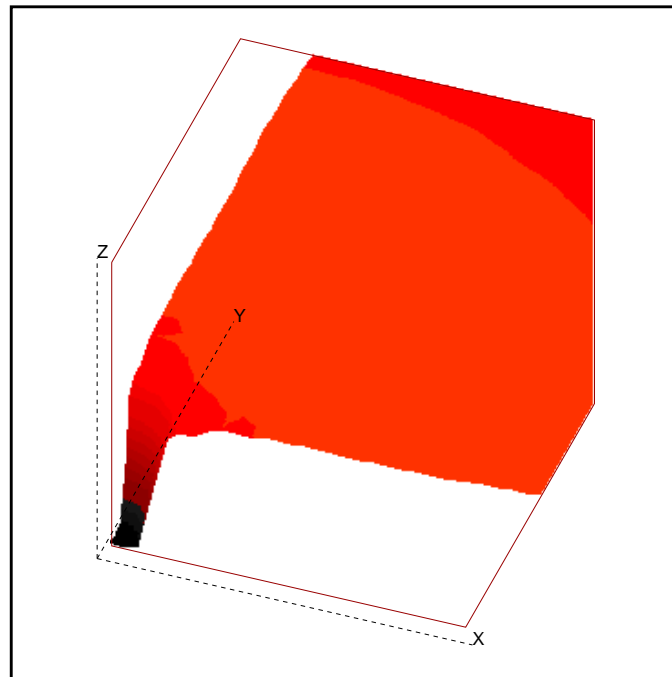
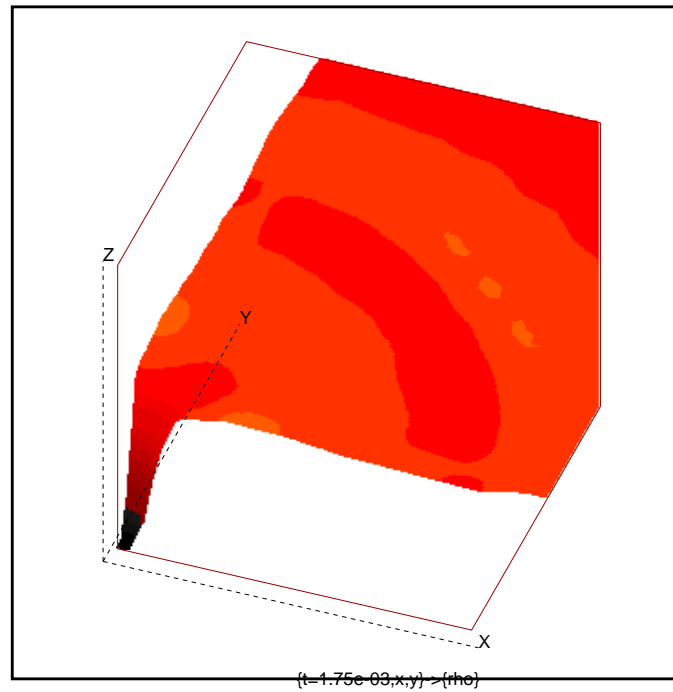
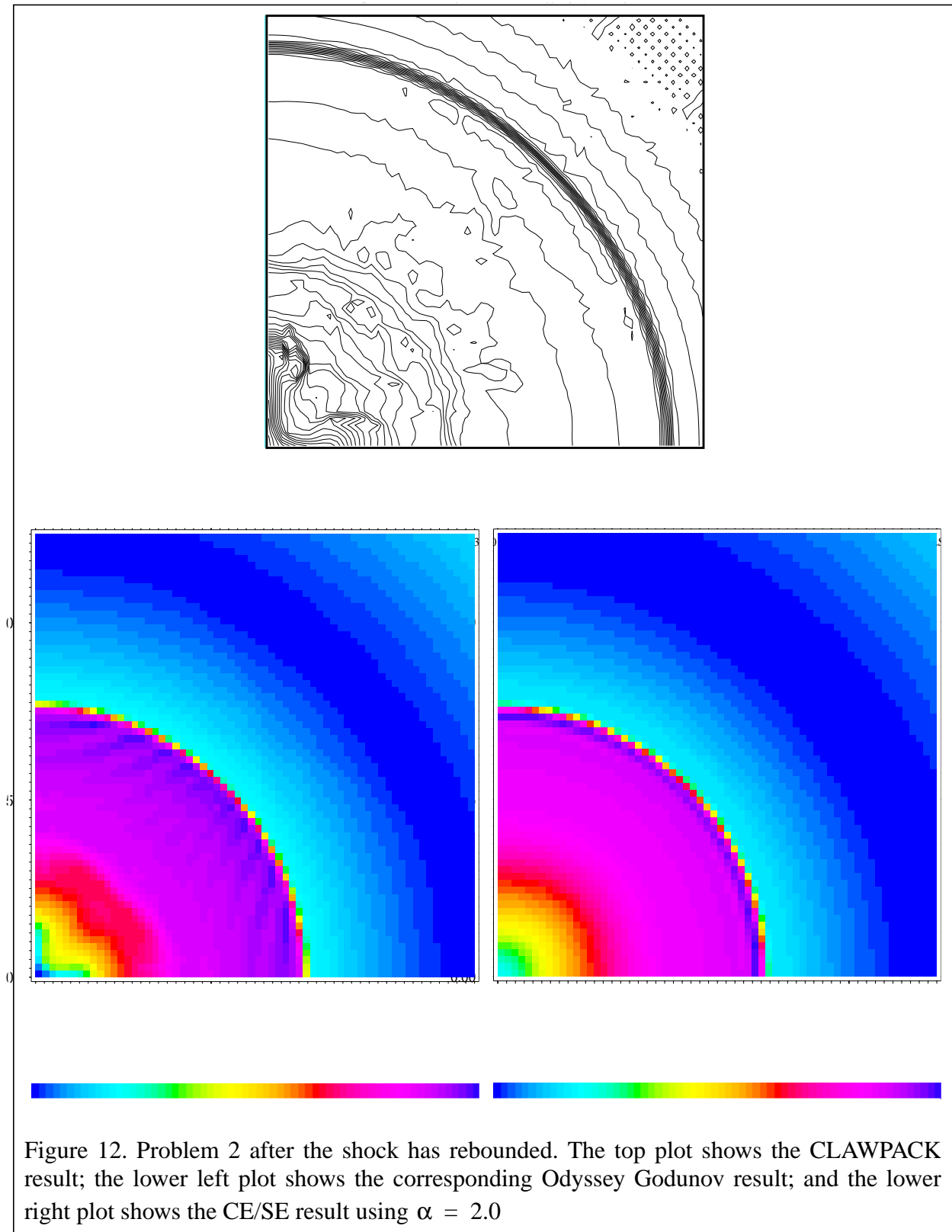
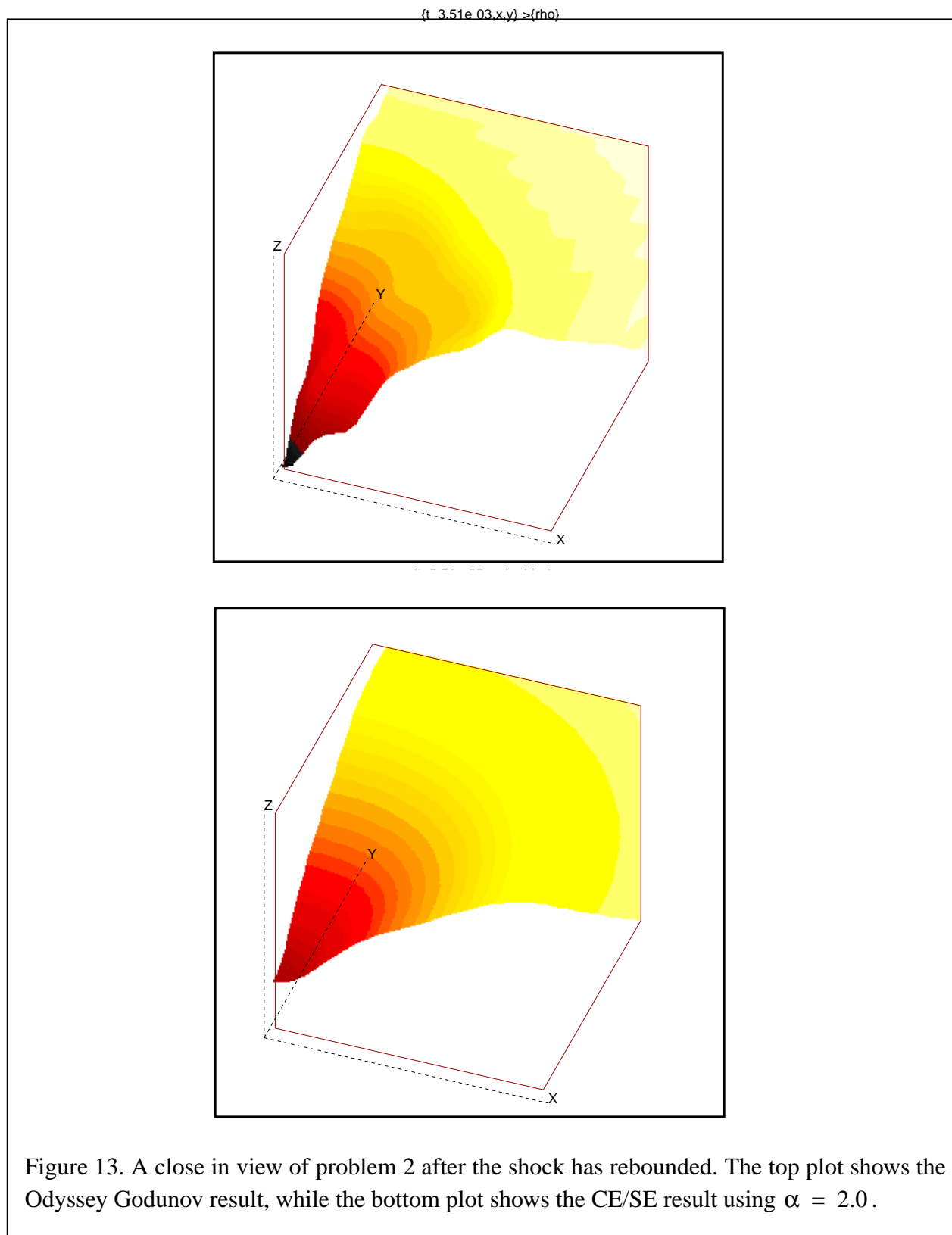


Figure 11. Close in views in problem 2 just before a major shock reaches the origin. The top plot shows the Odyssey Godunov result, while the bottom plot shows the CE/SE result using  $\alpha = 2.0$ .





effect. For the CE/SE method, mesh imprinting may have caused one contour to be slightly flattened. In this case, color contour plots only show a slight asymmetry in the solution.

A short while after the main shock bounce, the Godunov solutions in Figures 12 and 13 both show significant deterioration near the origin. In this case, jetting occurs on the coordinate axes near the origin, although not as pronounced as in the three region problem. As before, the CE/SE solution appears to be cylindrically symmetric.

These results establish beyond a doubt that the genuinely unsplit CE/SE technique is quite powerful. Using a square Cartesian grid, curved shocks are propagated almost without distortion across a grid that at no point in the simulation matches the shape of the shocks. It is also clear that very serious errors can arise due to the use of dimensional splitting in solvers of nonlinear equations. From our experience, the evidence points to the dimensional splitting errors becoming visible when the curvature of a shock becomes large in a single zone of the grid.

## Conclusions

The cylindrically symmetric shocks that propagate on a Cartesian grid are not distorted when the CE/SE solver is used. On the other hand, there is distortion when a Godunov method is used. In particular, there is a flattening of the shock about the  $x=y$  diagonal ( $x$  and  $y$  are the two Cartesian coordinates). In addition, there are errors in the position of the shock along the  $x$  and  $y$  axes.

The CE/SE method is a very promising new numerical method. There has been some confusion about its relation to other techniques. First, the method for finding a non-dissipative solution to the conservation laws is totally new. However, the formulation of the dissipation terms does draw upon other methods. Thus, while CE/SE is not a finite difference or a finite volume method, finite differences are used to compute the dissipation terms that damp the ringing at the shocks.

The ramifications of our results are not limited to the case when a shock has curvature. Any nonuniform flow, particularly one developing instabilities or turbulence, will be more faithfully followed by a technique like the CE/SE method. This method's genuinely unsplit character is critical to its accuracy in the tests presented here and points clearly to its potential in more demanding flow problems.

## Acknowledgments

This work was performed under the auspices of the U. S. Department of Energy by the Lawrence Livermore National Laboratory, under contract number W-7405-ENG-48.

## References

- S. C. Chang, "The Method of Space-Time Conservation Element and Solution Element - A New Approach for Solving the Navier-Stokes and Euler Equations," *J. Comput. Phys.* **119**, 295 (1995).
- S. C. Chang, X. Y. Wang, and C. Y. Chow, "The Method of Space-Time Conservation Element and Solution Element - Applications to One-Dimensional and Two-Dimensional Time-Marching Flow Problems," AIAA paper 95-1754, presented at the 12th AIAA Computational Fluid Dynam-

ics Conference, San Diego, California, June 19-22, 1995.

S. C. Chang, X. Y. Wang, and C. Y. Chow, "The Space-Time Conservation Element and Solution Element Method - A New High-Resolution and Genuinely Multidimensional Paradigm for Solving Conservation Laws I. The Two-Dimensional Time Marching Schemes," 1998, submitted.

P. Colella, "A Direct Eulerian MUSCL Scheme for Gas Dynamics", *SIAM J. Sci. Comput.* **6** (1), 104 (1985).

W. Dai and P. R. Woodward, "A Second-Order Unsplit Godunov Scheme for Two- and Three-Dimensional Euler Equations," *J. Comput. Phys.* **134**, 261 (1997).

L. A. Khan and P. L.-F. Liu, "Numerical analyses of operator-splitting algorithms for the two-dimensional advection-diffusion equation," *Comput. Methods Appl. Mech. Engrg.* **152**, 337 (1998).

R. J. LeVeque, "Wave Propagation Algorithms for Multidimensional Hyperbolic Systems," *J. Comput. Phys.* **131**, 327 (1997).

M. V. Papalexandris, A. Leonard, P. E. Dimotakis, "Unsplit Schemes for Hyperbolic Conservation-Laws with Source Terms in One Space Dimension," *J. Comput. Phys.* **134**, 31 (1997).

J. Saltzman, "An Unsplit 3D Upwind Method for Hyperbolic Conservation Laws," *J. Comput. Phys.* **115**, 153 (1994).